

Global Topological Changes of Offset Domains

Weishi Li
School of Instrument Science
Hefei University of Technology
Hefei, China
Weishi.Li@hotmail.com

Ralph R Martin
School of Computer Science and Informatics
Cardiff University
Cardiff, UK
ralph@cs.cf.ac.uk

Abstract—Offsetting is used in a range of CAD/CAM applications, such as tool path generation for pocket machining. In many applications, topological changes caused by offsetting are undesirable, and should be prevented, or detected. We present methods based on the medial axis transform to determine when a topological change may occur under an inward offset, an outward offset, or a combination of both, for a domain bounded by Jordan curves.

In other applications, such as morphological image processing, a combination of outward and inward offsets are used to deliberately change the topology of a domain, e.g. to close small gaps in a region. Such an operation may fail to change the topology if certain conditions are not satisfied. We show how to detect such cases, and how to modify the domain's medial axis transform to achieve the intended topological change.

Keywords-Topology; Offset curve; Medial axis transform; Closing; Opening

I. INTRODUCTION

An *offset curve* is a curve a fixed distance away from a *progenitor curve*. In this paper, we take the progenitor curve to be a *Jordan curve*: a plane curve which is topologically equivalent to a circle, in other words, simple and closed. A connected planar domain may be bounded by several nested curves. We call the domain bounded by the progenitor curves the *progenitor domain*. The domain resulting by offsetting these curves consistently (inwards or outwards) with respect to the progenitor domain is called the *offset domain*. The topology of the offset domain may differ from that of the progenitor domain, so, for example, the inward offset domain of a singly-connected domain may comprise several parts. Such topological change may be undesirable: an example arises when computing tool paths for pocket machining [1]. In this paper, we employ the medial axis transform (MAT) [2] to describe the shape of a connected bounded domain in \mathbf{R}^2 , and to analyse topological change when offsetting domains.

Computing an offset curve of a given curve is not a trivial problem. In general, the offset curve is not a rational parametric curve even if the given curve is a polynomial parametric curve. Much effort has been put into approximating offset curves [3]; Farouki and Sakkalis [4] introduced Pythagorean hodographs curves, a special kind of spline admitting rational offsets. Offset curves may self-intersect

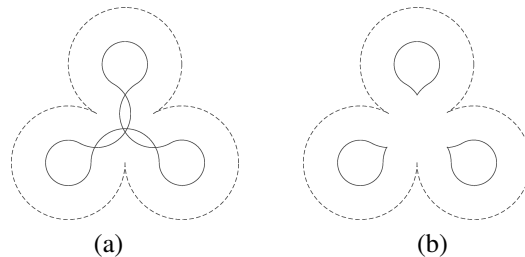


Figure 1. (a): an offset curve, (b): the corresponding trimmed offset curve. Here and in other figures the progenitor curve is shown as a dashed line, and the offset curve is a solid line.

(see Figure 1(a)) or intersect with the offsets of other progenitor curves if more than one progenitor curve is given. Thus, parts of the offset curve may need to be removed to get the trimmed offset curve (see Figure 1(b)), which is often referred to simply as the offset curve for short. A formula that expresses the genus of the offset in terms of the degree and genus of the original curve is given by Arrondo et al [5]. Trimming the offset curve is tricky [6], [10]. In pocket machining, the *Voronoi diagram*, which is closely related to the medial axis for a simple curve composed of circular arcs and line segments, may be used to compute the offset curve without use of a troublesome trimming process [6], [8], [9]. Distance maps may also be used to trim offset curves when the progenitor curve is a free-form curve [7].

Exact computation of the medial axis is tricky, so various algorithms have been designed to compute an approximation of the MAT, especially for a domain with free-form curved boundaries [11], [12], [13], [14], [15], [16]. A review of algorithms for MAT generation is given in [17].

A novel approach to computing the MAT is given by Choi et al [18], [19], [20], [15]. The basic idea is to decompose the complicated domain into a set of simple and easy-to-handle sub-domains, and to compute the MAT for each sub-domain. The MAT of the complicated domain is then the union of the MATs of the sub-domains. A similar idea was presented by Chiang [21] independently. Choi et al further study domain decomposition from the viewpoint of offsets, and use it to compute offset curves [20]. An algorithm for computing offset curves using the MAT is also given in [16].

Existing research on curve offsetting is mainly concerned with *geometric* aspects of the problem, and considerations of topology have focused on how to produce a *trimmed* offset curve with correct topology [20], [?], [22]. In contrast, in this paper, we analyse the *global topological change* which may occur when a domain is offset inwards or outwards, or when a combination of these operations is used; we also consider how to control topological change. The boundary of the domain is presumed to be a Jordan curve, or several nested Jordan curves. A domain bounded by one curve is *singly-connected*, while a domain bounded by several nested curves is *multiply-connected*. We do not consider algorithms for MAT generation, as they can be found elsewhere. Simple examples are used in this paper to explain topological changes in the domain for different offset operations.

This paper significantly extends some ideas originally presented in [23]. Section II gives various results about MATs and offsetting. Topological changes for inward and outward offsetting are analysed in Sections III and IV, respectively. Combined inward and outward offsetting is analysed in Section V. Conclusions are given in Section VI.

II. PRELIMINARIES

Let Ω be a connected and bounded domain in \mathbf{R}^2 , and $\partial(\Omega)$ be its boundary, comprising a finite number of nested Jordan curves. The *medial axis* [11], [18], [21] of Ω is the locus of centers of maximal inscribed circles within Ω . The MAT of Ω is denoted $\mathcal{M}(\Omega)$ and comprises the medial axis plus the associated radius $r(\mathbf{p})$ at each point \mathbf{p} of the medial axis. A domain can be reconstructed from its MAT, i.e.

$$\Omega = \mathcal{M}^{-1}(\mathcal{M}(\Omega)),$$

where

$$\mathcal{M}^{-1}(\mathcal{M}(\Omega)) = \{\mathbf{q} \mid \|\mathbf{p}, \mathbf{q}\| \leq r(\mathbf{p}), \forall (\mathbf{p}, r(\mathbf{p})) \in \mathcal{M}(\Omega)\},$$

and $\|\cdot, \cdot\|$ denotes Euclidean distance.

A domain Ω and its medial axis are homotopically equivalent, i.e. if Ω is n -connected, its medial axis is also n -connected. The maximal inscribed circle centered at \mathbf{p} contacts $\partial(\Omega)$ at certain points. Non-isolated contact points of a medial axis point constitute a circular contact arc. Taking an isolated contact point or a circular contact arc as a contact component, the number of contact components at any medial axis point is finite. If there is only one contact component, the point is an endpoint of the medial axis. If there are $n \geq 3$ contact components, the point is a bifurcation point of the medial axis [18]. If Ω is bounded by a finite number of mutually disjoint simple closed curves, each of which comprises a finite number of piecewise real analytic curves, the number of endpoints and bifurcation points of the medial axis of Ω is finite, and the bifurcation points break a medial axis into a finite number of curve segments [18]. The two endpoints of a single curve segment may meet at the *same* bifurcation point—see Figure 2(a). The MAT may also be a

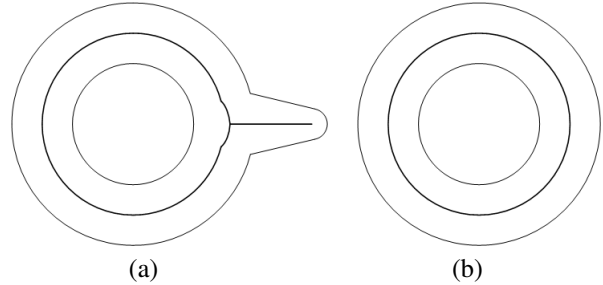


Figure 2. Medial axes of domains bounded by nested Jordan curves.

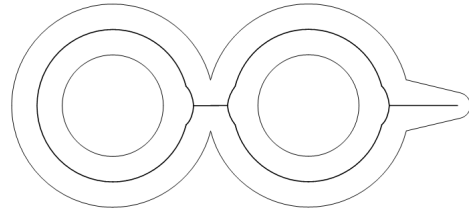


Figure 3. A domain bounded by three Jordan curves and its medial axis.

single closed curve—see Figure 2(b). If one endpoint of a medial axis edge is an endpoint, it is an open branch edge. A point \mathbf{p} is a locally maximal or minimal point of $\mathcal{M}(\Omega)$ if $(\mathbf{p}, r(\mathbf{p})) \in \mathcal{M}(\Omega)$ and $r(\mathbf{p})$ is locally maximal or minimal respectively. Bifurcation points of the medial axis of any domain bounded by Jordan curves must be locally maximal points [18]. The medial axis of a connected domain can be represented as a connected graph, whose vertices are the endpoints and bifurcation points, and whose edges are the curve segments.

For a multiply-connected domain Ω , the edges of its medial axis graph can be classified into three types (see Figure 3): (i) edges that constitute a cycle, (ii) edges that constitute a path connecting two cycles, and (iii) edges that constitute an open branch path connecting an endpoint of the medial axis and a cycle. A connecting path may also be part of another cycle, and cycles appear in the medial axis around each hole of Ω . In the medial axis shown in Figure 3, there are two cycles, one path connecting the two cycles and one branch path. If we prune the branch paths, the medial axis graph is still homotopically equivalent to the progenitor domain.

If the domain is bounded by non-Jordan curves, the bifurcation point of its medial axis may be locally a minimal point—see Figure 4(a); the medial axis may also be disconnected—see Figure 4(b).

The inward offset of Ω by a distance r is the set

$$\mathcal{O}_{-r}(\Omega) = \mathbf{R}^2 - \{\mathbf{p} \mid D(\mathbf{p}, \mathbf{R}^2 - \Omega) \leq r\},$$

and the outward offset of Ω with a distance r is the set

$$\mathcal{O}_{+r}(\Omega) = \{\mathbf{p} \mid D(\mathbf{p}, \Omega) \leq r\}.$$

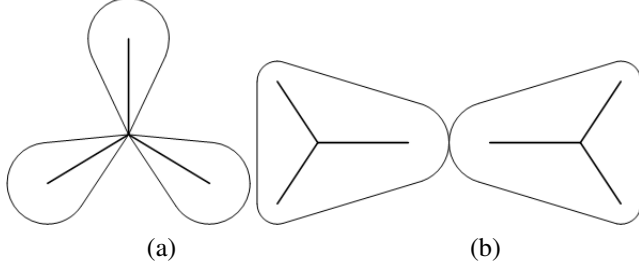


Figure 4. Domains bounded by non-Jordan curves and the medial axis.

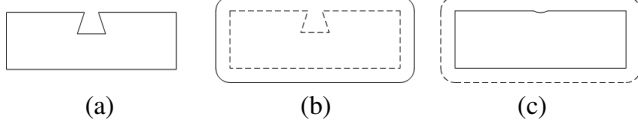


Figure 5. Closing operation: (a) progenitor curve; (b) outward offset curve; (c) the result of the closing operation.

Here $\{\mathbf{p} \mid D(\mathbf{p}, A) \leq r\}$ is the Minkowski sum of some domain A and a disk of radius r centered at \mathbf{p} .

Define

$$\mathcal{M}(\Omega)_{-r} = \{(\mathbf{p}, r(\mathbf{p}) - r) \mid (\mathbf{p}, r(\mathbf{p})) \in \mathcal{M}(\Omega)\}.$$

Then

$$\mathcal{M}(\Omega)_{-r} = \mathcal{M}(\mathcal{O}_{-r}(\Omega))$$

and furthermore

$$\mathcal{O}_{-r}(\Omega) = \mathcal{M}^{-1}(\mathcal{M}(\Omega)_{-r}).$$

This property can be used to compute inward offset curves [16], [20]. However, if we define

$$\mathcal{M}(\{\Omega_i\})_{+r} = \{(\mathbf{p}, r(\mathbf{p}) + r) \mid (\mathbf{p}, r(\mathbf{p})) \in \mathcal{M}(\{\Omega_i\})\},$$

in general the converse does not hold:

$$\mathcal{M}(\{\Omega_i\})_{+r} \neq \mathcal{M}(\mathcal{O}_{+r}(\{\Omega_i\}))$$

and

$$\mathcal{O}_{+r}(\{\Omega_i\}) \neq \mathcal{M}^{-1}(\mathcal{M}(\{\Omega_i\})_{+r}).$$

Thus, $\mathcal{O}_{+r}(\{\Omega_i\})$ can not be computed directly using $\mathcal{M}(\{\Omega_i\})$ as in the case for inward offset curves. We will show later in Section IV that in general, the medial axis of $\{\Omega_i\}$ is not a subset of the medial axis of $\mathcal{O}_{+r}(\{\Omega_i\})$.

We analyse the topological change between Ω and each of $\mathcal{O}_{-r}(\Omega)$ and $\mathcal{O}_{+r}(\Omega)$ in Sections III and IV respectively. Ω , $\mathcal{O}_{-r}(\mathcal{O}_{+r}(\{\Omega_i\}))$ and $\mathcal{O}_{+r}(\mathcal{O}_{-r}(\Omega))$ are in general not geometrically identical. In morphological image processing [24], $\mathcal{O}_{-r}(\mathcal{O}_{+r}(\{\Omega_i\}))$ is called a *closing operation* (see Figure 5), while $\mathcal{O}_{+r}(\mathcal{O}_{-r}(\Omega))$ is called an *opening operation* (see Figure 6). Note that closing may fill a concavity in the progenitor curve, while corners of the progenitor curve are rounded by opening.

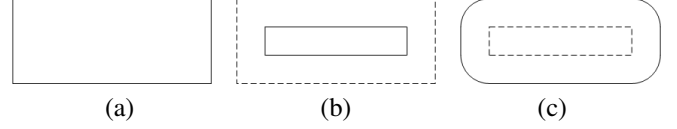


Figure 6. Opening operation: (a) progenitor curve; (b) inward offset curve; (c) the result of the opening operation.

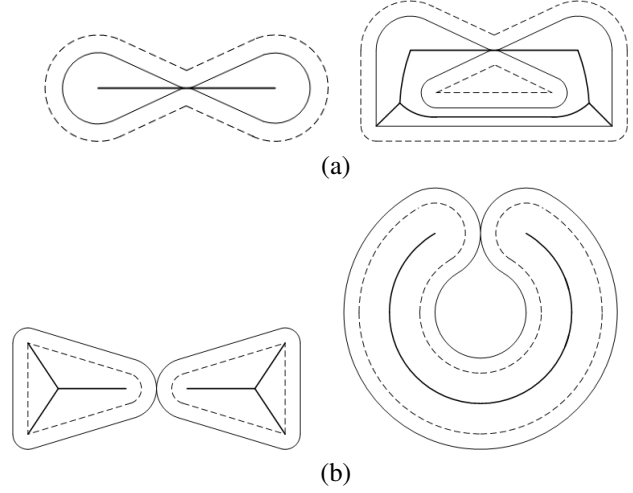


Figure 7. Critical cases for offsetting: (a) inward offset; (b) outward offset.

When a domain is offset, either outwards or inwards, or multiple domains are simultaneously offset outwards, the offset boundary curves may contact at various isolated points—for examples, see Figure 7. In these cases, the offset domain is considered to be homotopically equivalent to the progenitor domain. Note that this can not happen during closing or opening if the progenitor domain is bounded by Jordan curves.

III. INWARD OFFSETS

In this Section, we consider topological changes which may arise during inward offset of a singly-connected domain, and then of a multiply-connected domain. An example application of inwards offsetting is in pocket machining, where it is used to generate tool paths.

A. Singly-Connected Domains

There is no cycle in the medial axis of a singly-connected domain: the medial axis graph is a tree. As the connectedness of a domain can only be decreased after inwards offsetting, the topology of a singly-connected progenitor domain Ω can only change in one way: $\mathcal{O}_{-r}(\Omega)$ can be broken into several disconnected parts, and at the same time $\mathcal{M}(\mathcal{O}_{-r}(\Omega))$ is also broken into several disconnected parts.

There are two possibilities: one is that $\mathcal{M}(\mathcal{O}_{-r}(\Omega))$ is broken at an edge, and the other is that $\mathcal{M}(\mathcal{O}_{-r}(\Omega))$ is broken at a bifurcation point. Clearly, if any edge of $\mathcal{M}(\mathcal{O}_{-r}(\Omega))$ is broken into several parts (i.e. the radius

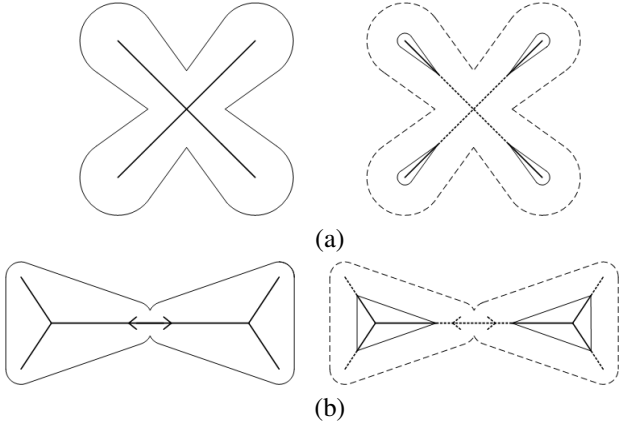


Figure 8. Inward offset of singly-connected domains(left: progenitor domain; right: offset domain).

function associated with the corresponding edge of the $\mathcal{M}(\Omega)$ is not less than r everywhere, and parts of the edges with associated radius bigger than r are not connected), $\mathcal{M}(\mathcal{O}_{-r}(\Omega))$ is no longer homotopically equivalent to $\mathcal{M}(\Omega)$, and in consequence $\mathcal{O}_{-r}(\Omega)$ is not homotopically equivalent to Ω .

When $\mathcal{M}(\mathcal{O}_{-r}(\Omega))$ is broken at the bifurcation point, there are two cases as illustrated in Figure 8. The medial axis of the offset domain is shown as a thick solid line, and the parts of medial axis of the progenitor domain where the associated radius function is less than r are shown as thick dashed lines in the offset domain (this convention is also used in subsequent figures). The medial axis $\mathcal{M}(\mathcal{O}_{-r}(\Omega))$ is broken into several parts, but no edge is broken into parts, if either of the following two conditions is satisfied:

- 1) The radius associated with at least one bifurcation point of $\mathcal{M}(\Omega)$ is less than the offset distance r , and simultaneously there are multiple incident edges whose associated radius functions are not strictly less than r —see Figure 8(a).
- 2) The radii associated with at least two bifurcation points of $\mathcal{M}(\Omega)$ are less than r , and simultaneously (i) there is at least one incident edge whose associated radius functions is not strictly less than r for each bifurcation point, and (ii) the radius function associated with the path between the two bifurcation points is strictly less than r —see Figure 8(b).

Here a path may comprise several edges of the medial axis graph. The topological change of a singly-connected domain may be a combination of these two possibilities. For any case of topological change, $\partial(\mathcal{O}_{-r}(\Omega))$ contains more curves than $\partial(\Omega)$, which is undesirable in pocket machining.

B. Multiply-Connected Domains

The bifurcation points of the medial axis of a multiply-connected domain can be classified into two kinds: (i)

bifurcation points whose incident edges are *all* parts of some open branch paths, and (ii) bifurcation points some of whose incident edges are parts of cycles or paths connecting two cycles.

As for singly-connected domains, $\mathcal{M}(\mathcal{O}_{-r}(\Omega))$ can be broken at an edge or a bifurcation point. For edges that constitute an open branch path and bifurcation points whose incident edges are all parts of some open branch paths, the topological change is the same as for a singly-connected domain. In other words, if edges and bifurcation points in the medial axis of a multiply-connected domain Ω satisfy the condition given in Section III-A, the topology of $\mathcal{O}_{-r}(\Omega)$ is different from that of Ω .

We now turn to edges and bifurcation points of other kinds, i.e. (i) edges that constitute a cycle, (ii) edges that constitute a path connecting two cycles, and (iii) bifurcation points whose incident edges are not all parts of some open branch paths. Clearly, if the radius associated with any point of a connecting path is less than r , $\mathcal{M}(\mathcal{O}_{-r}(\Omega))$ is no longer homotopically equivalent to $\mathcal{M}(\Omega)$. If the connecting path is also part of a cycle, the offset domain $\mathcal{O}_{-r}(\Omega)$ may still be connected, but the genus of $\mathcal{O}_{-r}(\Omega)$ differs from that of $\mathcal{M}(\Omega)$; otherwise, $\mathcal{O}_{-r}(\Omega)$ may be broken into several parts. The topology of $\mathcal{O}_{-r}(\Omega)$ may differ from that of Ω in six distinct ways, as illustrated in Figures 9(a)–(f) respectively:

- A cycle may break into at least two parts.
- A cycle may break into two branch paths. Note that, unlike the previous case, the offset domain has fewer boundary curves than the progenitor domain.
- A connecting path may break into at least two parts.
- At least two connecting paths which are also parts of another cycle may break.
- A connecting path which is also part of another cycle may break into at least two parts. Again, unlike the previous case, the offset domain has fewer boundary curves than the progenitor domain.
- The radius associated with a bifurcation point whose incident edges are not all parts of some open branch paths is less than r , and it does not matter what happens to the edges incident to the bifurcation point.

For the cases illustrated in Figure 9(a), (c), (d) and (f), $\mathcal{O}_{-r}(\Omega)$ must break into several parts. Such cases are undesirable in pocket machining, although other cases are acceptable, as $\partial(\mathcal{O}_{-r}(\Omega))$ contains fewer curves than $\partial(\Omega)$.

The topological change when inwardly offsetting a multiply-connected domain may include a combination of all possibilities given in this and the previous Section, dependent on the shape of the domain, or alternatively, its MAT. If no edge constitutes an open branch path connecting an endpoint of the medial axis and a cycle in the medial axis of the domain, the possibilities given in Section III-A can be excluded, and vice versa. The connectedness of a multiply-connected domain can decrease, or the domain may break into several disconnected sub-domains, after inwards

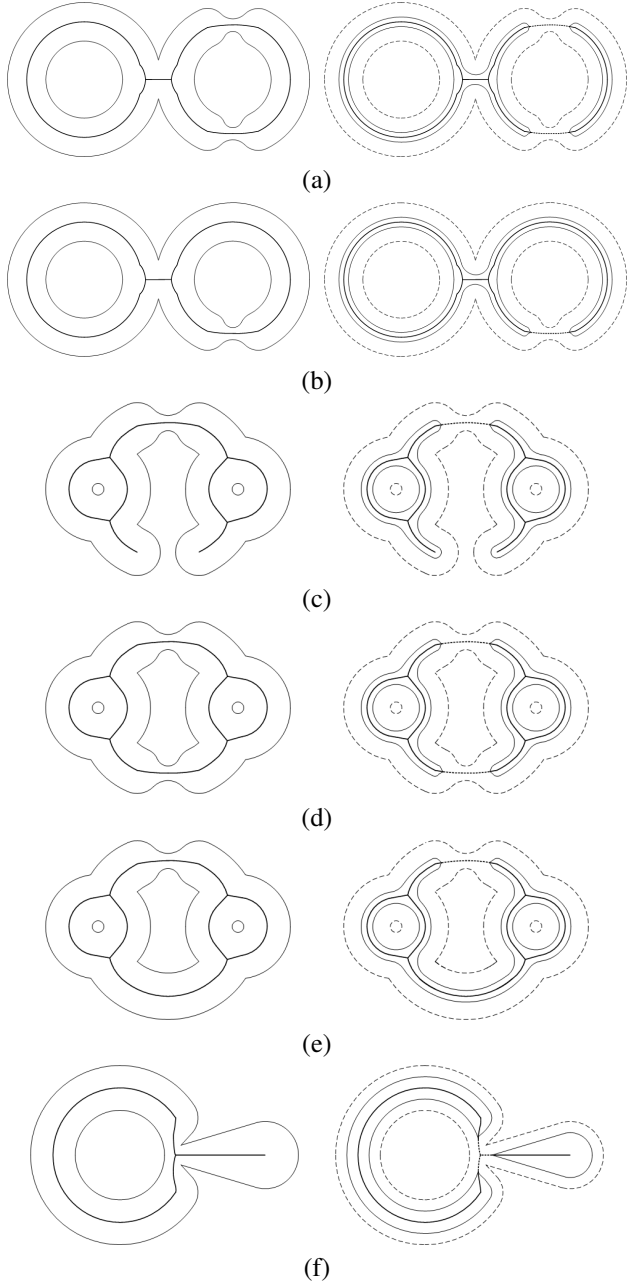


Figure 9. Inward offset of multiply-connected domains (left: progenitor domain; right: offset domain): (a) a cycle of the medial axis breaks into two pieces; (b) a cycle of the medial axis breaks into two branch paths; (c) a connecting path breaks into two pieces; (d) two connecting paths which are also parts of another cycle breaks; (e) a connecting path which is also part of another cycle breaks; (f) the radius associated with a bifurcation point is less than r .

offsetting. If a cycle breaks into two branch paths, or a connecting path which is also part of another cycle breaks into two parts, the connectedness of the offset domain is decreased by 1. If any of the other possibilities occurs, the offset domain breaks into several parts.

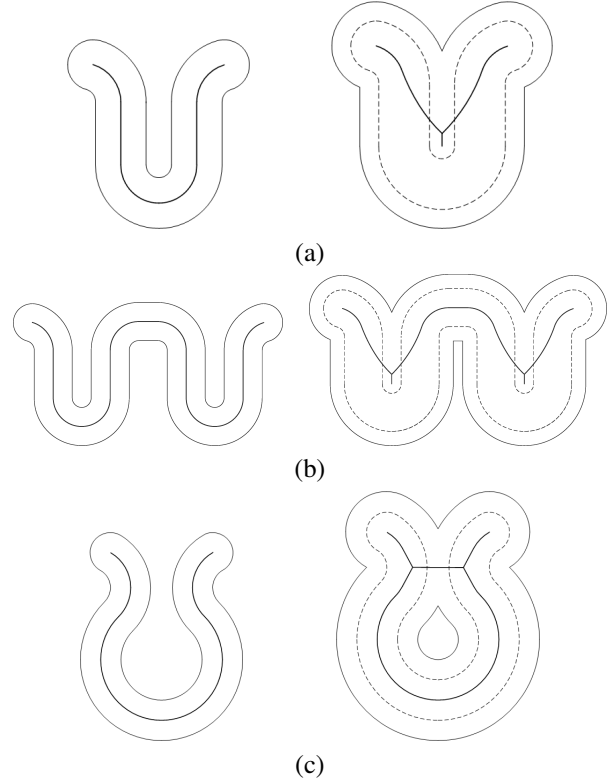


Figure 10. Outward offset of singly-connected domains. Left: progenitor domain, right: offset domain. Case (a) and (b): no topological change, (b): topological change.

IV. OUTWARD OFFSETS

In this Section, we consider topological change during outward offsetting of a domain or multiple domains. The connectedness of a domain can either decrease or increase: existing holes of the domain may be filled, and new holes may be created. However, the offset domain can not break into pieces.

Given one singly-connected domain Ω , if two distinct points \mathbf{p}_i and \mathbf{p}_j of $\mathcal{M}(\Omega)$ satisfy $\|\mathbf{p}_i\mathbf{p}_j\| < r(\mathbf{p}_i) + r(\mathbf{p}_j) + 2r$, then the circle with radius $r(\mathbf{p}_i) + r$ centered at \mathbf{p}_i and the circle with radius $r(\mathbf{p}_j) + r$ centered at \mathbf{p}_j intersect each other. If such points are continuous over $\mathcal{M}(\Omega)$ —see Figure 10(a), or continuous over several isolated parts of $\mathcal{M}(\Omega)$ —see Figure 10(b), $\mathcal{O}_{+r}(\Omega)$ is homotopically equivalent to Ω ; otherwise, new holes are created, and the topology of $\mathcal{O}_{+r}(\Omega)$ differs from that of Ω —see Figure 10(c).

Given a multiply-connected domain Ω , for an open branch path or a connecting path which is not a part of another cycle, the local topological change is same to that of a singly-connected domain.

We now turn to edges that constitute a cycle. If the distinct points \mathbf{p}_i and \mathbf{p}_j of $\mathcal{M}(\Omega)$ satisfying $\|\mathbf{p}_i\mathbf{p}_j\| < r(\mathbf{p}_i) + r(\mathbf{p}_j) + 2r$ constitute a whole cycle, the corresponding hole is filled, and $\mathcal{O}_{+r}(\Omega)$ is not homotopically equivalent to Ω —

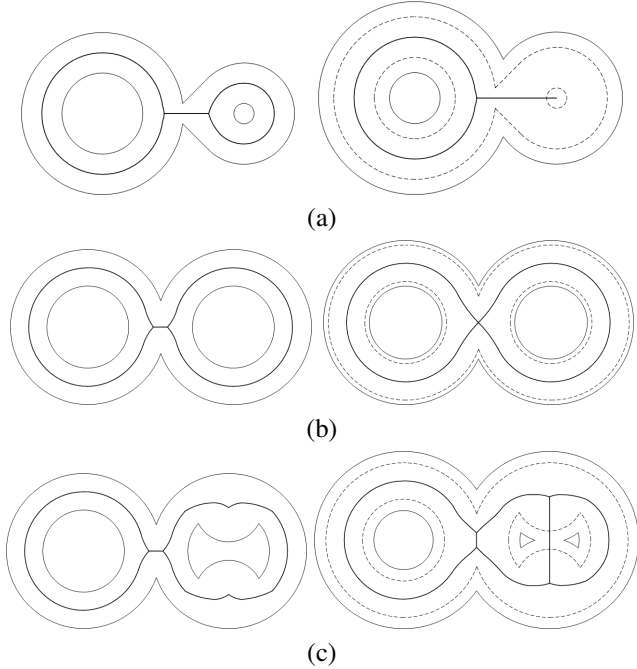


Figure 11. Outward offset of multiply-connected domains. Left: progenitor domain, right: offset domain. Case (a): gap filled, (b): no topological change, (c): one hole is broken into two holes.

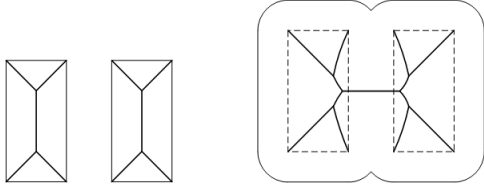


Figure 12. Outward offset of two initially separate domains (left: progenitor domain; right: offset domain)

see Figure 11(a). As for a singly-connected domain, if such points constitute a continuous non-full-cycle segment, which may have branches, $\mathcal{O}_{+r}(\Omega)$ is homotopically equivalent to Ω —see Figure 11(b); otherwise, if such points are not continuous, new holes are created, and the topology of $\mathcal{O}_{+r}(\Omega)$ differs from that of Ω —see Figure 11(c). The topological change for a multiply-connected domain may be a combination of all possibilities given in this Section.

For two domains, if $\|\mathbf{p}_i \mathbf{p}_j\| < r(\mathbf{p}_i) + r(\mathbf{p}_j) + 2r$ for two points \mathbf{p}_i and \mathbf{p}_j of the two medial axes respectively, the outward offsets of the two domains merge, causing topological change—see Figure 12.

Generally, the medial axis of Ω is not a subset of the medial axis of $\mathcal{O}_{+r}(\Omega)$, and $\mathcal{M}(\{\Omega_i\})_{+r} \neq \mathcal{M}(\mathcal{O}_{+r}(\{\Omega_i\}))$. As a result, $\mathcal{O}_{+r}(\{\Omega_i\}) \neq \mathcal{M}^{-1}(\mathcal{M}(\{\Omega_i\})_{+r})$.

V. COMBINATIONS OF INWARD AND OUTWARD OFFSETS

We next consider the topological caused by a combination of inward and outward offsets to one or several domains. We

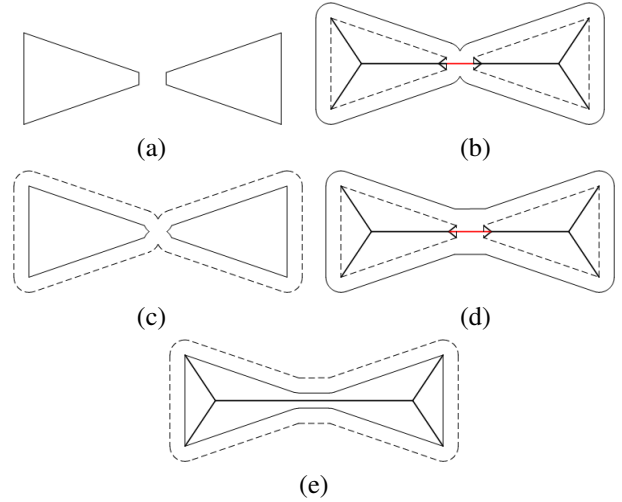


Figure 13. Closing two domains: (a) progenitor domains; (b) outward offset; (c) inward offset; (d) MAT adjustment and reconstruction; (e) new closing result.

follow the convention of morphological image processing to call $\mathcal{O}_{-r}(\mathcal{O}_{+r}(\Omega))$ and $\mathcal{O}_{+r}(\mathcal{O}_{-r}(\Omega))$ *closing* and *opening*, respectively.

A. Closing

Given a set of domains $\{\Omega_i\}$, a closing operation $\mathcal{O}_{-r}(\mathcal{O}_{+r}(\{\Omega_i\}))$ may be used with the intention of *closing* them. The closing operation fills in narrow gaps between the domains, joining them, as well as eliminating narrow concavities and small holes within each domain. If the width of a gap, a concavity or a hole is less than $2r$, it is filled by the operation $\mathcal{O}_{+r}(\{\Omega_i\})$. However, the subsequent inward offset operation may re-open some areas connected by the outward offset operation, as noted in [23]—see Figure 13. In Figure 13(b), two domains are merged by the outward offset operation as the minimum distance between the two progenitor domains is less than $2r$. However, inward offsetting in this case re-separates the two domains, as can be seen in Figure 13(c); solid lines denote the boundaries of the final result. This can be explained by considering $\mathcal{M}(\mathcal{O}_{+r}(\{\Omega_i\}))$. For $\mathcal{M}(\mathcal{O}_{+r}(\{\Omega_i\}))$, the radius associated with each medial axis point inside $\{\Omega_i\}$ must be bigger than r , with the exception that the radius associated with medial axis points on the boundary of $\{\Omega_i\}$ may be equal to r . Note that this is not necessarily true for any medial axis points outside $\{\Omega_i\}$. If there are points on $\mathcal{M}(\mathcal{O}_{+r}(\{\Omega_i\}))$ with associated radius less than r , $\mathcal{O}_{-r}(\mathcal{O}_{+r}(\{\Omega_i\}))$ will re-open the domain—see Figure 13(c). The thick black and red segments give the medial axis of $\mathcal{O}_{+r}(\{\Omega_i\})$; the red segment is outside $\{\Omega_i\}$ and a part of the red segment has associated radius less than r .

If segments of $\mathcal{M}(\mathcal{O}_{+r}(\{\Omega_i\}))$ have associated radius less than r , and at such points we modify the radius to

make it greater than r , reconstructing the domain using the new MAT guarantees a closed result after inward offsetting $\mathcal{O}_{+r}(\{\Omega_i\})$. We refer to segments of $\mathcal{M}(\mathcal{O}_{+r}(\{\Omega_i\}))$ that lie outside $\{\Omega_i\}$ and connect $\{\Omega_i\}$ as *connection segments*. Note that the radius functions associated with other parts of $\mathcal{M}(\mathcal{O}_{+r}(\{\Omega_i\}))$ must always be greater than r . Examining the radius function associated with the connection segments allows us to identify those where the newly connected region may become disconnected again by inward offsetting.

Along a connection segment, if the minimum associated radius is less than r , re-opening will occur during inward offsetting if nothing is done to prevent it—see Figure 13(c). We thus adjust the associated radius function of those connection segments where the associated radius is less than or equal to r .

In many applications, it is helpful to give the closing region a *natural shape*, which may be done as follows. Before adjusting the radii, each identified connection segment \mathcal{T} is extended in both directions along the medial axis—see Figure 13(d). The maximal inscribed circles associated with the extensions inside $\{\Omega_i\}$ allow us to determine new radii for each point of the segment in a suitable way. Each segment is extended to whichever comes first: either the nearest medial axis bifurcation point, or the first point \mathbf{p} along the medial axis satisfying $l = r(\mathbf{p}) - r$, where $r(\mathbf{p})$ is the radius associated with \mathbf{p} , and l is the distance from \mathbf{p} to the corresponding initial endpoint of the segment. If $\mathbf{p} \in \Omega_j (\Omega_j \subset \{\Omega_i\})$, \mathbf{p} is typically near an endpoint of $\mathcal{M}(\Omega_j)$. Thus, local shape information near the ‘tip’ of Ω_j is taken into account. As noted in Section IV, the medial axis of $\{\Omega_i\}$ is generally not a subset of the medial axis of $\mathcal{O}_{+r}(\{\Omega_i\})$, so \mathbf{p} does not exactly coincide with the endpoint of $\mathcal{M}(\Omega_j)$. The new radius function assigned to each extended connection segment \mathcal{T}' may be determined by linearly interpolating the associated radii at its two endpoints. After such adjustment, we obtain $\bar{\mathcal{M}}(\mathcal{O}_{+r}(\{\Omega_i\}))$, which is in places the same as $\mathcal{M}(\mathcal{O}_{+r}(\{\Omega_i\}))$. We thus define a *reliable closing operation* formally by

$$\hat{\mathcal{C}}_r(\{\Omega_i\}) = \mathcal{O}_{-r}(\mathcal{M}^{-1}(\bar{\mathcal{M}}(\mathcal{O}_{+r}(\{\Omega_i\}))).$$

A reconstruction result found by inverting the modified MAT is illustrated in Figure 13(d), and the corresponding reliable closing result is given in Figure 13(e). Because of radius re-assignment, the associated radius for any point of $\bar{\mathcal{M}}(\mathcal{O}_{+r}(\{\Omega_i\}))$ is greater than r . Thus, $\hat{\mathcal{C}}_r(\{\Omega_i\})$ and $\mathcal{O}_{+r}(\{\Omega_i\})$ are homotopically equivalent, and closing is guaranteed.

B. Opening

For a domain Ω , $\mathcal{O}_{+r}(\mathcal{O}_{-r}(\Omega))$ may be used with the intention of *opening* it. The opening operation suppresses small protrusions, and will cut a domain connected only by a narrow neck into two separate domains. Specifically, bumps or necks of width less than $2r$ are cut away from

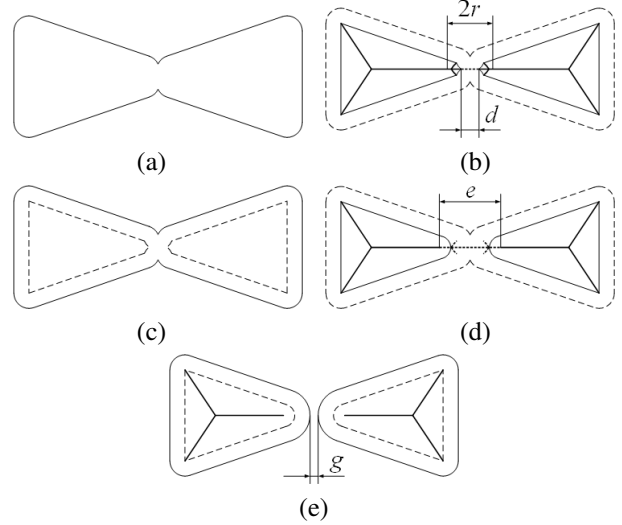


Figure 14. Opening a domain: (a) the progenitor domain; (b) the inward offset; (c) the outward offset; (d) MAT adjustment and reconstruction; (e) the new opening result.

$\mathcal{O}_{-r}(\Omega)$. However, the outward offset operation may re-close some areas opened by the inward offset operation—see Figure 14. In Figure 14(b), the domain is broken into two parts after the inward offset operation. As $d < 2r$, (here d is the distance between the two endpoints of the segment shown in dashed lines, and each point \mathbf{p} of the segment satisfies $r(\mathbf{p}) < r$), the outward offset re-closes the two regions, as shown in Figure 13(c). The existence of such a segment results in a failure to open the domain. In this specific example, $\mathcal{O}_{+r}(\mathcal{O}_{-r}(\Omega)) = \Omega$, as shown in Figure 14(c). In general, a segment $S \in \mathcal{M}(\Omega)$ which satisfies $r(\mathbf{p}) < r, \forall \mathbf{p} \in S$ may contain bifurcation points.

As suggested for closing, $\mathcal{M}(\mathcal{O}_{-r}(\Omega))$ can be adjusted to open the domain reliably. We can identify all cut-off points between medial axis segments $\{\mathcal{T}_i\}$ which satisfy $r(\mathbf{p}) < r, \forall \mathbf{p} \in \{\mathcal{T}_i\}$ and other segments. Note that such a cut-off point \mathbf{q} satisfies $r(\mathbf{q}) = r$; it cannot be a bifurcation point, as a bifurcation point is locally maximal. If any two cut-off points \mathbf{p}_i and \mathbf{p}_j exist for which $\|\mathbf{p}_i \mathbf{p}_j\| < 2r$, the outward offset will re-close the domain between \mathbf{p}_i and \mathbf{p}_j . Such a pair of cut-off points exist only if there is a path in $\{\mathcal{T}_i\}$ between them because $\mathcal{O}_{+r}(\mathcal{O}_{-r}(\Omega)) \in \Omega$ (otherwise, part of $\mathcal{O}_{+r}(\mathcal{O}_{-r}(\Omega))$ would lie outside Ω). To perform reliable opening, such paths are extended along $\mathcal{M}(\Omega)$ to label those medial axis segments whose associated radius function must be adjusted to open the domain. If no bifurcation point is encountered, the path is extended until $\|\mathbf{p}_s \mathbf{p}_e\| > r(\mathbf{p}_s) + r(\mathbf{p}_e) + 2r$, where \mathbf{p}_s and \mathbf{p}_e are the present endpoints of the path; otherwise, the path is extended along all edges incident to the bifurcation point until any pair of endpoints \mathbf{p}_s and \mathbf{p}_e in the two directions satisfies $\|\mathbf{p}_s \mathbf{p}_e\| > r(\mathbf{p}_s) + r(\mathbf{p}_e) + 2r$.

We simply prune the extended path from $\mathcal{M}(\mathcal{O}_{-r}(\Omega))$

except for its endpoints. After such adjustment, we have $\bar{\mathcal{M}}(\mathcal{O}_{-r}(\Omega))$, which is in places the same as $\mathcal{M}(\mathcal{O}_{-r}(\{\Omega_i\}))$. The domain will be opened at the corresponding position after outward offsetting—see Figure 14(e). This reliable opening operation is formally given by

$$\hat{\mathcal{O}}_r(\Omega) = \mathcal{O}_{+r}(\mathcal{M}^{-1}(\bar{\mathcal{M}}(\mathcal{O}_{-r}(\Omega)))).$$

VI. CONCLUSIONS

We have presented an analysis of the global topological changes which may occur when offsetting domains bounded by Jordan curves. When performing inward or outward offsets alone, we can predict topological change caused by offsetting, by analysing the medial axis transform. Morphological closing and opening operations performed using combinations of inward and outward offsetting are intended to introduce topological change. We have discussed conditions for when these operators fail to produce the desired topological change, and a method of modifying the medial axis transform to ensure the intended topological change is achieved in each case.

ACKNOWLEDGMENT

The first author is partially supported by National Natural Science Foundation of China (Grant No.: 61070125).

REFERENCES

- [1] B.K. Choi and R.B. Jerard, *Sculptured surface machining*, Dordrecht: Kluwer Academic Publishers, 1998.
- [2] H. Blum, A transformation for extracting new descriptors of shape, *Proc. Symp. Models for the Perception of Speed and Visual Form*, 362-380, 1967.
- [3] Nicholas M. Patrikalakis and Takashi Maekawa, *Offset Curves and Surfaces*, In *Shape Interrogation for Computer Aided Design and Manufacturing*, 293-365, 2002.
- [4] R.T. Farouki and T. Sakkalis, *Pythagorean hodographs*, *IBM Journal of Research and Development*, 34(5)(1990) 736-752.
- [5] Enrique Arrondo and Juana Sendra and J. Rafael Sendra, *Genus formula for generalized offset curves*, *Journal of Pure and Applied Algebra*, 136(3)(1999) 199-209.
- [6] Martin Held, *On the Computational Geometry of Pocket Machining*, Springer-Verlag, Berlin, 1991.
- [7] Joon-Kyung Seong and Gershon Elber and Myung-Soo Kim, *Trimming local and global self-intersections in offset curves/surfaces using distance maps*, *Computer-Aided Design*, 38(3)(2006) 183-193.
- [8] Martin Held, *Voronoi diagrams and offset curves of curvilinear polygons*, *Computer-Aided Design*, 30(4)(1998) 287-300.
- [9] Martin Held and Stefan Huber, *Topology-oriented incremental computation of Voronoi diagrams of circular arcs and straight-line segments*, *Computer-Aided Design*, 41(5)(2009) 327-338.
- [10] Joon-Kyung Seong, David E. Johnson, Gershon Elber, Elaine Cohen, *Critical point analysis using domain lifting for fast geometry queries*, *Computer-Aided Design*, 42(7)(2010) 613-624.
- [11] W. L. F. Degen, *Exploiting curvatures to compute the medial axis for domains with smooth boundary*, *Computer Aided Geometric Design*, 21(7)(2004) 641-660.
- [12] M. Ramanathan and B. Gurumoorthy, *Constructing medial axis transform of planar domains with curved boundaries*, *Computer-Aided Design*, 35(7)(2003) 619-632.
- [13] R. Dorado, *Medial axis of a planar region by offset self-intersections*, *Computer-Aided Design*, 41(12)(2009) 1050-1059.
- [14] J. Batista Oliveira and Luiz Henrique De Figueiredo, *Robust approximation of offsets, bisectors, and medial axes of plane curves*, *Reliable Computing*, 9(2)(2003) 161-175.
- [15] Hyeong In Choi and Chang Yong Han and Hwan Pyo Moon and Kyeong Hah Roh and Nam-Sook Wee, *Medial axis transform and offset curves by Minkowski Pythagorean hodograph curves*, *Computer-Aided Design*, 31(1)(2009) 59-72.
- [16] Lixin Cao and Jian Liu, *Computation of medial axis and offset curves of curved boundaries in planar domain*, *Computer-Aided Design*, 40(4)(2008) 465-475.
- [17] Dominique Attali and Jean-Daniel Boissonnat and Herbert Edelsbrunner, *Stability and Computation of Medial Axes — a State-of-the-Art Report*, In *Mathematical Foundations of Scientific Visualization, Computer Graphics, and Massive Data Exploration*, 109-125, 2009.
- [18] H.I. Choi and S.W. Choi and H.P. Moon, *Mathematical theory of medial axis Transform*, *Pacific Journal of Mathematics*, 181(1)(1997) 57-88.
- [19] Hyeong In Choi and Sung Woo Choi and Hwan Pyo Moon and Nam-Sook Wee, *New algorithm for medial axis transform of plane domain*, *Graphical Models and Image Processing*, 59(6)(1997) 463-483.
- [20] H.I. Choi and S.W. Choi and C.Y. Han and T.-W. Kim and S.-H. Kwon and H.P. Moon and K.H. Roh and N.-S. Wee, *Two-dimensional offsets and medial axis transform*, *Advances in Computational Mathematics*, 28(2)(2008) 171-199.
- [21] C.-S. Chiang, *The Euclidean distance transform*, PhD Thesis, Purdue University, West Lafayette, 1992.
- [22] Juan Gerardo Alcazar and Juan Rafael Sendra, *Local shape of offsets to algebraic curves*, *Journal of Symbolic Computation*, 4232007 338-351.
- [23] Weishi Li and Ralph R. Martin and Frank C. Langbein, *Merging and smoothing machining boundaries on cutter location surfaces*. *ACM SPM 2010*, 165-170.
- [24] Jean Serra, *Image Analysis and Mathematical Morphology*, Academic Press, 1984.